Design of Shape Memory Alloy Spring Actuator for Pinch Valve Actuation

Manikandan N[a]., Kanchana, J[a], Siva Sankar M[a], Radhakrishnan P[b]
[a]*Department of Mechanical Engineering,PSG College of Technology, Coimbatore-641004,India*
[b]*PSG Institute of Advanced Studiesy,Coimbatore-641004,India*

Abstract

In this study, an analytical model to determine the force-deflection characteristics of SMA compression springs was developed. The developed model was verified experimentally for SMA compression springs of different sizes. Based on this study the design of a Shape Memory Alloy (SMA) spring actuator was carried out. The study was extended to the modelling of the pinch or squeeze force to control the flowing fluid in a flexible tube. The results of the modelling studies were corroborated by experiments on a silicone tube of 2 mm inner diameter and 4 mm outer diameter.

Nomenclature

SMA	Shape Memory Alloy
FRL	Filter Regulator Lubricator unit
D	mean diameter of SMA spring (mm)
D	wire diameter of SMA spring (mm)
C	spring index of SMA spring
n	number of active coils in SMA spring
F	axial force (N).
G_a	shear modulus at 100% Martensite (N/mm^2)
M	bending moment of SMA Spring (N-mm)
E	Young's Modulus of the SMA material (N/mm^2)
I	moment of inertia (mm^4),
T	torsional moment (N-mm)
J	polar moment of inertia (mm^4)

Symbols

α	initial pitch angle of SMA spring (degree)
δ	deflection of SMA spring (mm)
ν	Poisson's ratio

1. Introduction

Pinch valves are employed in controlling fluid flow for micro fluidics, micro chemistry, sensors and implantable drug delivery systems [1].The pinch valves have advantages such as multiple choices of valve function and tubing materials, minimal pressure drop and no direct contact with the flowing fluid.

With the above mentioned advantages, determining the force required to squeeze the tube is an important parameter to design a pinch valve. This study focuses on the experimental determination of the squeeze force that varies with the pressure exerted by the fluid flowing through the tube. There are many ways of actuation of pinch valves. One of the techniques for actuation of pinch valves is the use of Shape Memory Alloys (SMAs). However the use of SMA for the pinch valve actuation has not been adequately studied. This paper documents the theoretical calculation of the actuation force when SMA is used in the form of a helical coil spring.

A Shape Memory Alloy (SMA) is able to memorize and recover its original shape, after it has been deformed by heating over its transformation temperature. This unique effect of returning to an original geometry after a large inelastic deformation (near 8%) is known as the shape memory effect (SME). SMAs have been widely proposed as actuators, in fields such as robotics, biometrics and Microsystems [2]. Shape memory alloys, especially Nitinol have gained popularity in medical devices because of their biocompatibility and fatigue resistance [3]. With the advantages of being a light weight technology and high power/weight ratio, SMAs are a viable

alternative to conventional actuators. Nitinol is commercially available in the form of wires, strips and tubes. Using the SMA in the form of wire is the simplest way to use it as an actuator for an application. But the design has the disadvantages of having a small stroke and large recovery force .As a tradeoff between force and stroke, the SMAs can be designed to be used as actuators in the form of springs which will depend only on geometrical factors [4].

2. MODELING OF SMA SPRING

Adelaide Nespoli et al. [5] gave a comprehensive review on the research work done in the field of SMA spring actuators. The review consisted of details of the SMA spring actuators developed by T.Ishii [6], Jansen et al. [7], Pulnev et al. [8] and Donnellan's improvement to the Stratasys Research and Applied Physics Laboratory mini actuator [9].

Alberto Bellini et al. [10] developed a SMA spring actuator for the operation of automobile tumble flaps. The actuator consists of two sets of SMA springs working as mutual antagonists to produce linear movement of an output shaft. Christopher G. Stevens [11] developed a SMA spring actuator based on conventional spring design and an Excel spreadsheet application was developed by him enabling an easy way to design SMA springs. Sonia Degeratu et al. [12] developed a Visual Basic application for the design of SMA spring actuators based on thermal analysis and conventional spring design. Igor Spinella and Eugenio Dragoni [13] compared the characteristics of solid and hollow SMA compression springs in which the spring design was based on conventional spring design.

M Follador et al. [4] developed a general method for the design of SMA spring actuators which was also based on conventional spring design. The work of Sung Min An et al. [14], who developed a two-state static model for the development of SMA spring actuators differ from the conventional spring design. The work considered four different parameters namely SMA spring mean diameter (D), the wire diameter (d), the pitch angle (α) and the number of active coils (n). Based on this work, a similar model was developed for SMA compression springs and the Force-Deflection characteristics were determined.

The disadvantages of conventional spring design is that only the linear elastic region is considered for design and the design ignores the fact that the SMA springs can retain the original shape even at a shear strain of 6% to 8% [14]. The equations developed by Sung Min An et al. [14] for SMA extension springs were studied and were used in the derivation of Force-Deflection relationships for SMA compression springs. The torsion and bending moments are also considered for the SMA compression spring design and are illustrated in Fig. 1(a) and Fig. 1(b) respectively.

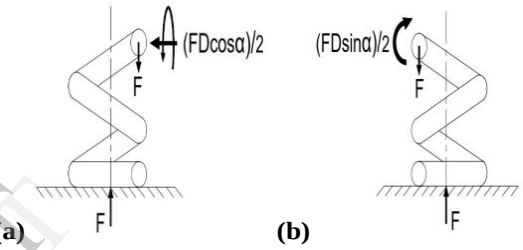

Fig.1. Moments in SMA compression springs (a) Torsional moment and (b) Bending moment.

According to spring design theory, springs undergo increase in mean diameter (D), when subjected to compression. The SMA spring under compressive load and its deflection based on pitch angle (α) is shown in Fig. 2.

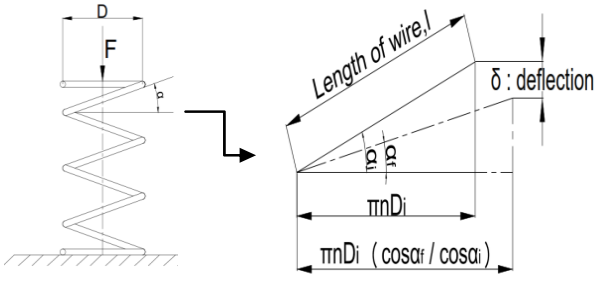

Fig. 2. Deflection of SMA spring under compression

The bending moment (M) and torsional moment (T) acting on the SMA spring are given by Eq. (1) and Eq. (2) respectively. The relationship between the deflection (δ) of the load and the axial force (F) follows from Castigliano's theorem which is given in Eq. (3).

$$M = (FD\sin\alpha)/2 \quad (1)$$

$$T = (FD\cos\alpha)/2 \quad (2)$$

$$\delta = \frac{\partial U}{\partial F} = \frac{1}{2}\int_{length}\frac{M^2}{EI}\,dl + \frac{1}{2}\int_{length}\frac{T^2}{GJ}\,dl \quad (3)$$

The mean spring diameter of a compression spring is likely to increase with large deformation. From Fig. 2 the increased diameter is given as a function of initial diameter as follows,

$$D_f = D_i(\cos\alpha_f / \cos\alpha_i) \quad (4)$$

On the simplification of Eq. (1),(2),(3) and (4), we get the relationship between force (F) and deflection(δ) and the spring diameter increase as follows,

$$\delta = \frac{8FD_f^3 n}{d^4\cos\alpha_f}\left(\frac{\cos^2\alpha_f}{G} + \frac{2\sin^2\alpha_f}{E}\right) \quad (5)$$

The deflection in Eq. (5) can be replaced by function of pitch angle using the kinematic relationship from Fig. 2 and Eq. (4) as follows,

$$\delta = \frac{\pi D_i^3 n}{\cos\alpha_i}(\sin\alpha_i - \sin\alpha_f) \quad (6)$$

With Eq. (6), the force-deflection-pitch angle relationship in (5) can be rearranged as force-pitch angle relationship as follows,

$$F = \frac{\pi d^4 G}{8D_i^2}\left(\frac{(\cos^2\alpha_i(\sin\alpha_i - \cos\alpha_f)}{\cos^2\alpha_f(\cos^2\alpha_f + \frac{\sin^2\alpha_f}{(1+\nu)})}\right) \quad (7)$$

The shear stress (τ) for the outer diameter of a coil spring can be derived easily from the axial force when the stress distribution across the cross section of the coil spring is linear. It is given by the Eq. (8).

$$\tau = \frac{8CF}{\pi D^2} \quad (8)$$

The shear strain for the spring can be obtained by replacing the 'F' in Eq. (7) with 'τ' from Eq. (8) and rearranging the result to $\tau = G\gamma$.

$$\gamma = \frac{1}{C}\left(\frac{(\cos^2\alpha_i(\sin\alpha_i - \cos\alpha_f)}{\cos^2\alpha_f(\cos^2\alpha_f + \frac{\sin^2\alpha_f}{(1+\nu)})}\right) \quad (9)$$

According to Brinson's thermo mechanical model [15], at high temperature (Austenite linear region 100%) state, considering only the linear region and at the low temperature (Martensite 100% region) state the shear stress equations are given as follows,

$$\tau = G_a\gamma \quad (10)$$

$$\tau = G_m\gamma \quad (11)$$

For the 100% Austenite state at high temperature, Eq. (6), (7), (8) and (9) were combined and rearranged as a force and deflection relationship using Eq. (10):

$$F = \frac{G_a d^4}{8D^3 n}\left(\left(\frac{\cos^3\alpha_i}{\cos^2\alpha_f(\cos^2\alpha_f + \frac{\sin^2\alpha_f}{(1+\nu)})}\right)\right)\delta \quad (12)$$

For the 100% Martensite state at low temperature, Eq. (6), (7), (8) and (9) were combined and rearranged as a force and deflection relationship using Eq. (11):

$$F = \frac{G_m d^4}{8D^3 n}\left(\left(\frac{(\cos^3 \alpha_i}{\cos^2 \alpha_f (\cos^2 \alpha_f + \frac{\sin^2 \alpha_f}{(1+\nu)})}\right)\right)\delta \quad (13)$$

2.1 Experimental verification of the model

The model was verified experimentally with the Force-Deflection characteristics of three SMA springs of different parameters. The three sample Ni-Ti SMA springs had the austenite finish temperature of 55 ^{0}C, 65 ^{0}C and 90 ^{0}C.The parameters of the SMA springs taken for experiment are given in Table 1.

Fig. 3 SMA springs used for verification of the model

Table 1.Parameters of SMA springs taken for experiment

Parameter	Unit	Sample 1	Sample 2	Sample 3
Number of active coils, n	-	5	5	7
Diameter of wire, d	mm	1.2	0.8	1.5
Mean diameter of the spring, D	mm	6.8	5.2	11.5
Spring index, C	-	5.67	6.5	7.67
Initial pitch angle, α_i	degree	6.5	10.0	7.0

An experiment was conducted to plot the force-deflection characteristics of thee SMA springs to determine the force deflection characteristic. The schematic of the experimental apparatus as shown in Fig. 4 consists of a small temperature chamber which is heated by a hot air blowing device. The temperature inside the chamber was controlled by the use of a thermostat. The thermostat cuts off the supply to the hot air blowing device when the preset temperature is reached. A load cell was used to measure the force that is being applied to compress the SMA springs. The SMA springs were compressed using a fine pitch screw. Once the spring was compressed to a particular predefined length, the reaction force was read using the Load cell with a digital display. The process was repeated for different deflection values and for three different SMA springs and the results were plotted. The results were compared with the developed analytical model and plotted in a graph as shown in Fig. 5(a) and Fig. 5(b).

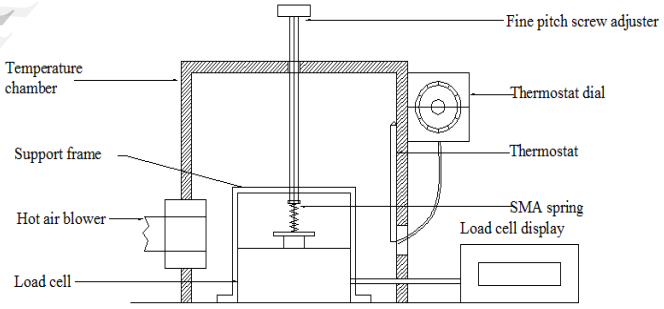

Fig. 4. Schematic of the experimental apparatus for determining the Force-Deflection characteristics of the SMA springs

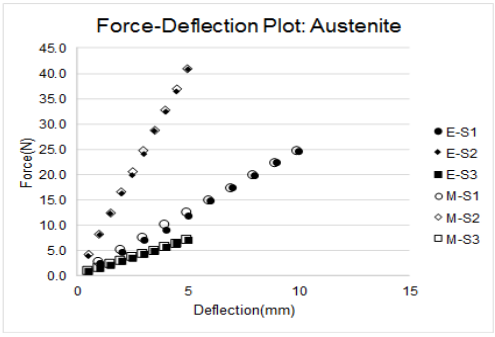

Fig. 5 (a) Comparison of force-deflection values from experiment and the developed model at the Austenite phase

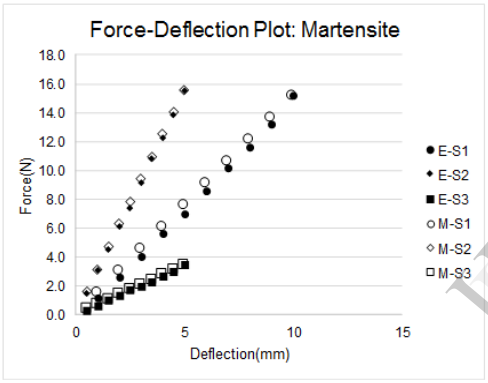

Fig. 5 (b) Comparison of force-deflection values from experiment and the developed model at the Martensite phase

The experiment was conducted until the shear strain reaches a value of 0.01. This shear strain value was selected to satisfy the condition that the SMA has to be operated within this range to get one million cycles of operation [16]. It can be seen from the graphs that the experimental and the model results correlate with each other with the less percentage of deviation. So, the developed model can be used for the design of springs for a specified actuation force.

The force required to squeeze the silicone tube shut was predicted using finite element analysis and the results were compared with the force values determined with an experimental apparatus.

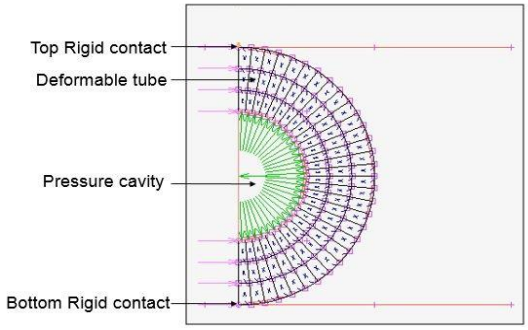

Fig. 6. FEA Model used for the analysis

2.2 Finite element analysis

Finite element analysis was carried out to determine the squeeze force using MSC Marc. The silicone tube was modeled as an elastomer with non-linear behavior [2]. The simulation was approximated to a plane strain problem to save computation time. The Ogden model is frequently used in FEA to simulate the behavior non-linear elastomers. The Ogden Elastomer model with large strain is used to simulate the deformation, stress and strain behavior of the silicone tube [2]. Since the problem is formulated as a plane strain one, Element type 80 in the User Library was chosen for meshing. It is a four node, isoparametric, quadrilateral element. It can be used for either small strain or large strain behavior using Mooney and Ogden models. The pressure of fluid flow is modeled as a closed cavity inside the tube's inner diameter. Element 171 is used. It is a 2-node, 2-D cavity element which can be used for plane strain and plane stress problems.

Contact analysis controlled by load was used to determine the squeeze force. Friction between the tube and the contact surfaces were also considered. The material parameters were input into the model as Stress-Strain history. The entire FEA model illustrated in Fig. 6.

Different pressure values were applied to the pressure cavity and the corresponding normal force at the top rigid contact was found. This normal force is equivalent to the force required to squeeze the tube. These values are shown in Table 2.

Table 2. Air Pressure and their corresponding squeeze force values by Finite Element Analysis.

Pressure (bar)	Force(N)		
	90 Elements	250 Elements	1000 Elements
0.20	3.20	3.12	3.10
0.40	5.50	4.70	4.61
0.60	6.70	6.63	6.47
0.80	8.73	8.67	8.57
1.00	10.93	10.83	10.76
1.20	13.36	13.10	13.06
1.40	16.05	15.59	15.58
1.60	19.04	18.36	18.35
1.80	22.35	21.42	21.42
2.00	25.98	24.80	24.80

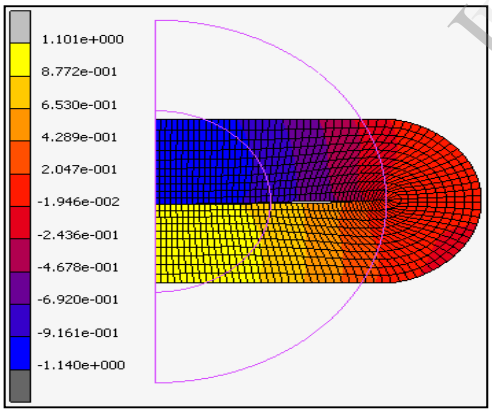

Fig.7 (a) Displacement in the silicone tube at 2 bar pressure

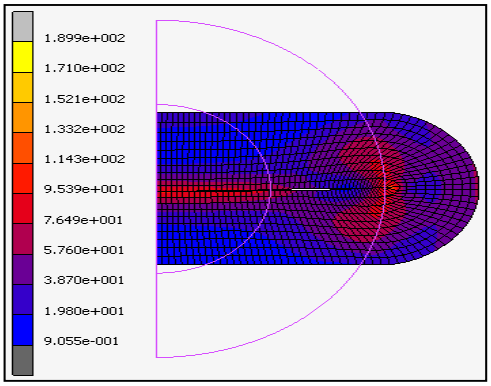

Fig.7 (b) Stress distribution in the silicone tube at a 2 bar pressure

Fig. 7(a) and 7(b) show the contour plots from finite element analysis of the silicone tube. The results show that the tube closes completely at a force of 24.98 N at a maximum pressure of 2 bar. The maximum shear stress in the tube is also found to be within the maximum shear strength of the silicone tube.

2.3 Experimental study and results

An apparatus was fabricated to determine the squeeze force experimentally. The apparatus consists of a Load Cell from PCB Piezotronics which is connected to a digital display meter. A support frame in the form of a channel is made from acrylic sheet to hold the silicone tube in position. One end of the silicone tube was connected to a FRL unit which supplies air and is passed through the support frame attached to the Load Cell as shown in Fig.8. The other end of the tube is attached to a flow meter. The force required to block the flow of fluid through the tube is applied by the rotational motion of the fine adjustment screw.

The experiments were carried out in the pressure range of 0.2 bar to 2 bar. The corresponding load values are noted from the load cell display. The force required to squeeze the silicone tube at various pressure values are tabulated as shown in Table 3.

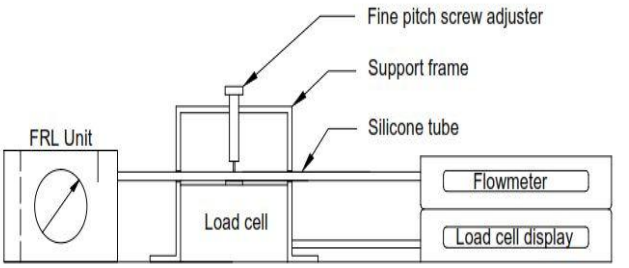

Fig. 8. Schematic of the experimental apparatus to determine the squeeze force

Table 3. Pressure and their corresponding squeeze force values from experiment.

Pressure (bar)	Force(N)			
	Experiment -Load values			
	Trial 1	Trial 2	Average	Force
0.20	0.35	0.34	0.35	3.38
0.40	0.50	0.48	0.49	4.81
0.60	0.72	0.74	0.73	7.16
0.80	0.88	0.81	0.85	8.29
1.00	1.18	1.25	1.22	11.92
1.20	1.30	1.33	1.32	12.90
1.40	1.43	1.48	1.46	14.27
1.60	1.61	1.80	1.71	16.73
1.80	1.92	2.10	2.01	19.72
2.00	2.34	2.28	2.31	22.66

Fig. 9 shows the Regression analysis graph and the relationship between the pressure and the force required to block the flow of air through the silicone tube. Polynomial curve fitting was used to determine the equation governing the variation of squeeze force with pressure. With the help of the equation, the squeeze force required to close the silicone tube at different pressure values can be predicted. Results from experiment and finite element analysis were compared and the values of force appear to be in close agreement.

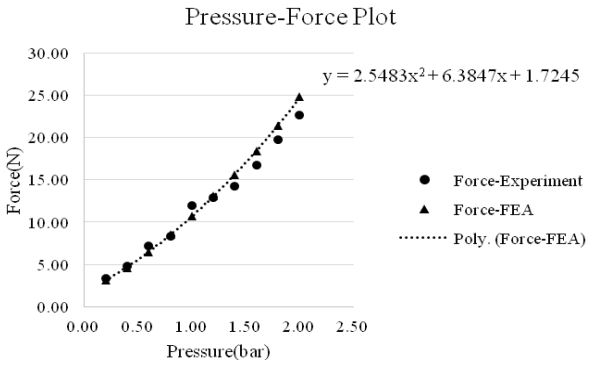

Fig. 9. Pressure vs. Squeeze force plot for the results from experiment

3. DESIGN OF THE SMA SPRING

From the results of the squeeze force analysis through FEA and experiment, it was found that the maximum force of 25 N is needed to close the silicon tube completely. But the spring was designed to exert a force of 33 N since the spring has to be used against a bias spring of 8 N. Once the model was verified with three different SMA springs of different spring parameters, a design of experiments was carried out using Taguchi L27 array orthogonal array to optimize the design of the spring. The optimized parameters of the SMA spring for the required force are tabulated in Table 4

Table 4. Optimized parameters of the SMA spring

Parameter	Value
Number of active coils, n	5
Diameter of wire, d	1.5 mm
Mean diameter of the spring, D	6.8 mm
Spring index, C	4.53
Initial pitch angle, α_i	6.5^0
Shear modulus, G_a	23.90 GPa
Shear modulus, G_m	9.56Pa

4. FINITE ELEMENT ANALYSIS OF THE DESIGNED SPRING

The finite element analysis of the optimized SMA spring was carried out in the commercially available MSC Marc Mentat non-linear analysis package. The SMA spring was modeled with the required parameters in NX 8.0 and imported into the Marc package as Parasolid file. The spring was meshed with tetrahedral (tet4) elements with an element size of 0.5 initially. A coupled electrical-thermal-structural analysis was carried out on the SMA spring. Element type 135 was used for the structural analysis and element type 134 was used for the thermal analysis. Two contact surfaces have been created to compress the spring. The position of the top surface was controlled to apply displacement and the bottom surface was constrained without movement. The finite element model of the spring is illustrated in Fig.10.

A temperature of 30^0C was applied as initial condition on all the nodes of the spring. A temperature of 80^0C was applied as the boundary condition so that the spring is maintained above the austenite finish temperature at the final load step. The material properties, initial and final boundary conditions are shown in Table 5.

Table 5 Mechanical and Thermal properties of the SMA used in FEA

Type	Shape Memory
Model	Thermomechanical
Young's Modulus	
Austenite	52827 N/mm^2
Martensite	21679 N/mm^2
Poisson's Ratio	0.33
Thermal Properties	
Martensite Start Temperature	55 ^{0}C
Martensite Finish Temperature	40 ^{0}C
Austenite Start Temperature	65 ^{0}C
Austenite Finish Temperature	75 ^{0}C

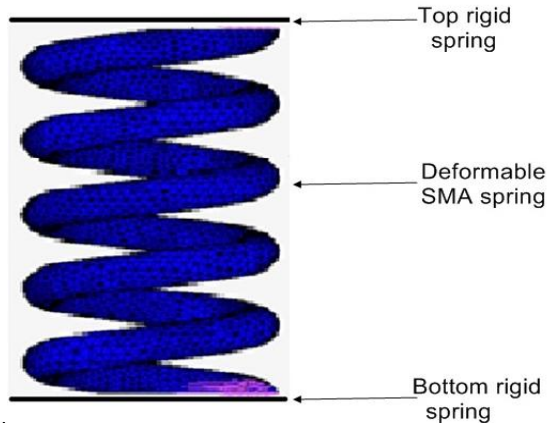

Fig. 10 Finite Element Model of the SMA spring

The martensite volume fraction, temperature distribution and the deflection of the SMA spring in FEA are shown in Fig. 11. In the analysis, the initial volume fraction of martensite was set to be 100%. The volume fraction of martensite reduces to zero showing transformation from martensite to austenite phase. The temperature distribution plot shows that the actuator achieves the austenite phase transformation temperature uniformly which will result in the actuation of the spring actuator. The deflection plot shows that the SMA spring actuator gets deflected to the designed stroke value at the austenite finish temperature.

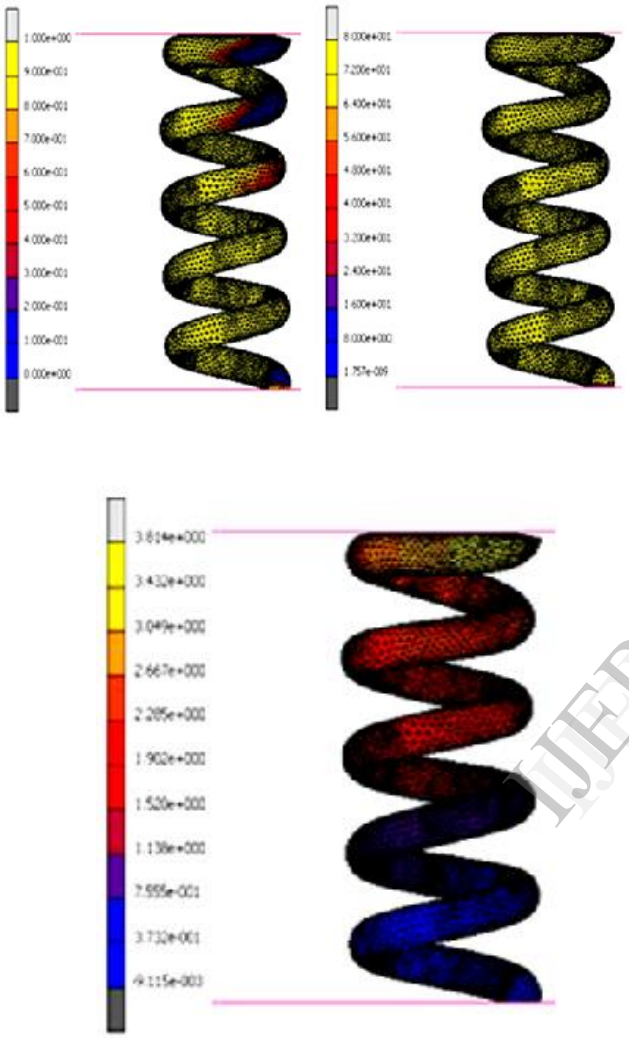

Fig. 11 Volume fraction of Martensite, Temperature distribution and deflection of the SMA spring in finite element analysis

4.1 Comparison of Finite element and experimental results

The analysis was repeated with element sizes of 0.3 and 0.1 until convergence is achieved.The Force-Deflection values of the designed SMA spring was found and compared with FEA and the conventional design results. The results are tabulated in Table 6 and plotted in Fig. 12 (a) and 12 (b).

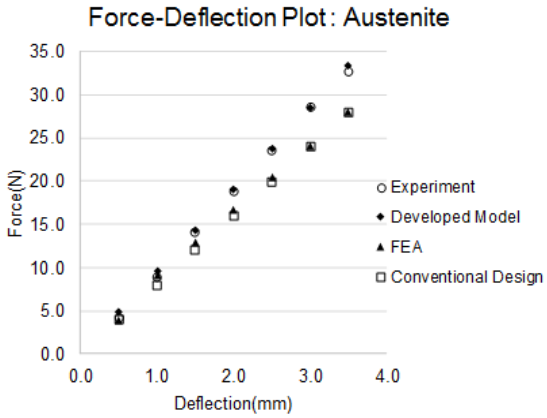

Fig. 12 (a) Comparison of the Force-Deflection plot at Austenite Phase

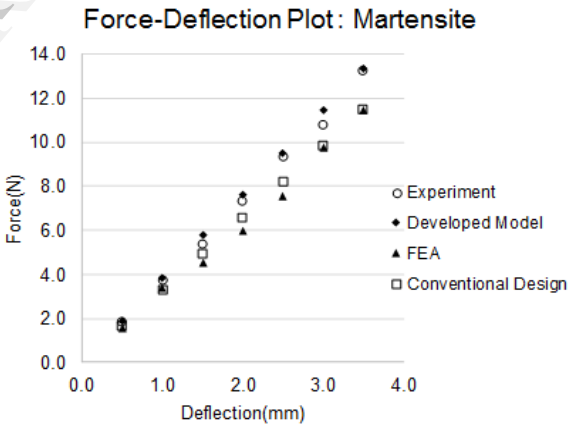

Fig. 12(b) Comparison of the Force-Deflection plot at Martensite Phase

Table 6 Comparison of Force-Deflection results from Experiment (E), Model (M), FEA and conventional spring desing (CD)

Deflection (mm)	Force (N)						Force (N)					
	Austenite						Martensite					
	E	M	%D	FEA	CD	%D	E	M	%D	FEA	CD	%D
0.5	4.2	4.8	12.1	4.0	4.0	5.3	1.9	1.9	2.6	1.6	1.6	13.4
1.0	9.0	9.6	6.4	9.1	8.0	12.0	3.7	3.8	2.4	3.4	3.3	13.7
1.5	14.1	14.3	2.0	12.9	12.0	17.2	5.4	5.8	6.6	4.6	4.9	9.8
2.0	18.9	19.1	1.3	16.7	16.0	18.0	7.4	7.6	3.2	6.0	6.6	12.2
2.5	23.5	23.8	1.2	20.5	20.0	17.8	9.3	9.5	2.2	7.6	8.2	13.7
3.0	28.6	28.6	0.1	24.1	24.0	19.1	10.8	11.4	5.6	9.8	9.8	9.7
3.5	32.6	33.3	2.0	28.1	28.0	16.6	13.2	13.3	0.6	11.4	11.5	15.4

5. Results and discussion

The application of SMA spring for pinch valve application was discussed. An analytical model was developed to determine the force-deflection characteristics of the SMA spring at 100% Austenite and 100% Martensite phases and the model was verified with SMA springs of different parameters. The results showed that the developed model can be used to determine the maximum force that can be achieved from a SMA compression spring at a particular deflection. The force required to close a silicone tube completely was predicted using finite element analysis and the results were compared with results from experiment. A force of 25 N was determined as the force required to close the tube completely at a pressure of 2 bar with air as the flow medium. Based on the maximum force required, a SMA spring actuator was designed to exert a force of 33 N since the spring has to work against a bias spring of 8N. The force values for a range of deflection values for the designed SMA actuator were determined and the results were compared with the force results from the conventional spring design and FEA. The results were improved and the error percentage was reduced from an average of 15% to 3.5% in the Austenite phase and from an average of 12.5% to 3.5% in the Martensite phase.From these results, it can be shown that the developed model can be used to determine the force-deflection characteristics of any SMA spring with different design parameters. The data obtained will be useful in the design of pinch valves using SMAs.

Acknowledgement

The authors thank Mr. Thomas Reininger, Festo AG & Co. KG, Germany for providing the materials this project.

References

[1] Catherine M. Pemble, Bruce C. Towe, 1999. "A miniature shape memory alloy pinch valve", Sensors and Actuators, Science Direct journals 77, pp. 145–148.

[2] Experimental elastomer analysis: MSC Software Corporation.

[3] Santa Clara, CA 1997, "Shape Memory Applications Inc., Introduction to Shape Memory and Superelasticity".

[4] Follador, M., Cianchetti, M., Arienti, A., and Laschi, C., 2012. "A general method for the design and fabrication of shape memory alloy active spring actuators", Smart Mater. Struct. 21, pp. 10.

[5] Adelaide Nespoli, Stefano Besseghini, Simone Pittaccio, Elena Villa, Stefano Viscuso, 2010. "The high potential of shape memory alloys in developing miniature mechanical devices: A review on shape memory alloy mini-actuators", Sensors and Actuators 158, pp. 149-160.

[6] Ishii, T., 2007, "Combinations and applications of bias method", Proceedings on SMST.

[7] Jansen, S., Breidert, J., Welp, E.G., 2004, "Positioning actuator based on shape memory wires", 9th International Conference on New Actuators.

[8] Pulnev, S., Vahhi, I., Priadko, A., Rogov, A., 2004, "Miniature linear actuators based on Cu–Al–Ni shape memory single crystals", Proceedings on SMST.

[9] Final report 2005, "Design and Testing of Linear Shape Memory Alloy Actuator", National Science Foundation – Research Experience for Undergraduates, summer 2005.

[10] Alberto Bellini, Marcello Colli, Eugenio Dragoni, 2009. "Mechatronic Design of a Shape Memory Alloy Actuator for Automotive Tumble Flaps: A Case Study", IEEE transactions on Industrial Electronics, 56.

[11] Christopher G Stevens, 1998. "Designing shape memory alloy springs for linear actuators", Springs Magazine.

[12] Sonia Degeratu, Nicu G. Bizdoaca, Gheorghe Manolea, Ilie Diaconu, Anca Petrisor, Vasile Degeratu,2008. "On the Design of a Shape Memory Alloy Spring Actuator Using Thermal Analysis", WSEAS Transactions on Systems 7, pp. 1006-1015.

[13] Igor Spinella, Eugenio Dragoni, 2010. "Modeling, Prototyping, and Testing of Helical Shape Memory Compression Springs with Hollow Cross Section", Journal of Mechanical Design 132.

[14] Sung-Min An, Junghyun Ryu, Maenghyo Cho, and Kyu-Jin Cho, 2011. "Engineering design framework for a shape memory alloy coil spring actuator using a static two-state model", Smart materials and structures 21, pp. 16.

[15] Brinson L C, 1993. "One-dimensional constitutive behavior of shape memory alloys: thermo-mechanical derivation with non-constant material functions and redefined Martensite internal variable", Journal of Intelligent Materials, Smart Systems and Structures.

[16] Dimitris.C.Lagoudas, Springer 2008, "Shape Memory Alloys: Modeling and Engineering Applications", pp.1- 40.